

RECENT RESULTS FROM TWO NEW AIRCRAFT-BASED FOURIER-TRANSFORM INTERFEROMETERS: The Scanning High-resolution Interferometer Sounder and the NPOESS Atmospheric Sounder Testbed Interferometer

H.E. Revercomb, V.P. Walden, D.C. Tobin, J. Anderson, F.A. Best, N.C. Ciganovich,
R.G. Dedecker, T. Dirks, S.C. Ellington, R.K. Garcia, R. Herbsleb, R.O. Knuteson, D.
LaPorte, D. McRae, and M. Werner

Space Science and Engineering Center
University of Wisconsin-Madison

1. Introduction

The Scanning High-resolution Interferometer Sounder (S-HIS) and the National Polar-orbiting Operational Environmental Satellite System (NPOESS) Atmospheric Sounder Testbed Interferometer (NAST-I) are new aircraft-based instruments that measure accurate infrared radiances at both high spectral and spatial resolution. The designs of both instruments are based upon the High-resolution Interferometer Sounder (HIS) and the ground-based Atmospheric Emitted Radiance Interferometer (AERI). However, both the new instruments are capable of cross-track scanning, which is important for the retrieval of atmospheric profiles of temperature, water vapor and other trace gases in the presence of clouds. The data from these instruments will be used to simulate future operational satellite sounders to evaluate their instrument specifications, measurement characteristics, and data-processing techniques.

This paper provides a brief description of each instrument, followed by an explanation of a general approach to correcting for detector nonlinearities. Preliminary data from the S-HIS, taken during the third Convection and Moisture Experiment (CAMEX-3), are compared with radiative transfer model calculations.

2. Instrument Characteristics

Both instruments use calibration sources that are based on those developed for the AERI; they are scaled-down (62%) versions. The AERI system has been compared with a reference blackbody maintained by the National Institute of Standards and Technology (NIST) to within 0.05 K for source temperatures ranging from ambient to 40 K above ambient; the comparison at ambient radiance was within 0.02 K.

2.1 Scanning High-resolution Interferometer Sounder

The S-HIS was initially designed to fly aboard an unmanned aircraft vehicle (UAV) with limited payload capacity. Therefore, it is small and light-weight, and has low power requirements. The S-HIS is a Fourier-transform interferometer with laser-controlled sampling. It utilizes a mechanical detector cooler, eliminating the use of cryogen. Due to the initial design constraints on size, the S-HIS uses a novel "3-color" detector with a shared focal plane, eliminating the need for multiple detectors and their associated dichroic beamsplitters and coolers. The S-HIS design and performance parameters are given in Table 1.

The S-HIS utilizes a 45° scene mirror that rotates through a measurement sequence consisting of views of the earth and two calibration sources, one at ambient and another up to 60 K above ambient. The raw interferograms from each view are compressed in real time to reduce the volume of data. A numerical filter is applied using a digital signal processor (DSP), while a second DSP is used for controlling the instrument. The S-HIS uses calibration techniques that were developed for the HIS and AERI (Revercomb *et al.*, 1988).

The retrieval and spectroscopic applications of the S-HIS data require high radiometric accuracy. The RMS noise level in terms of brightness temperature for the AERI and HIS instruments is generally less than 0.2 K, except near the edges of spectral bands and in some localized spectral regions. The performance of the S-HIS is comparable for its shorter dwell time, except for the extra longwave (ELW) band which requires longer averaging times for comparable performance.

Between August and December 1998, the instrument flew aboard both NASA's DC-8 research

aircraft as part of the third Convection and Moisture Experiment and on NASA's ER-2 aircraft during a NOAA-K validation campaign off the coast of California. It has the potential to fly on a UAV and other aircraft in the future as opportunities arise.

2.2 NPOESS Atmospheric Sounder Testbed Interferometer

The NAST-I was built by Massachusetts Institute of Technology (MIT) Lincoln Labs to perform atmospheric measurements for NPOESS. The interferometer is designed to provide high spectral resolution, low noise data from the NASA ER-2 aircraft (20 km) suitable for evaluating data of potential future satellite-borne sounders, such as AIRS, CRIS, and IASI. The collecting and scanning optics provide a 7.5-degree field-of-view (2.6 km nadir footprint) over a cross-track field of ± 48.2 degrees. This spatial resolution, combined with high spectral resolution, will permit the testing of proposed cloud handling algorithms and define the degradation in product accuracy expected to occur with decreasing satellite sensor spatial resolution. The radiometric accuracy of NAST-I will also permit full spatial resolution soundings and studies of the trade-off between spatial resolution and radiometric noise on sounding vertical resolution and accuracy using data collected under realistic atmospheric conditions.

Table 2 lists various specifications of the NAST-I. Refer to Cousins and Smith (1999) for a more detailed account of the instrument design and operation. The NAST-I has participated in several field experiments including the Wallops '98 campaign out of Wallops Island, Virginia and CAMEX-3.

3. Longwave Detector Nonlinearity

The longwave and midwave detectors (HgCdTe) of both the S-HIS and NAST-I exhibit nonlinear behavior. This is a saturation effect where as the incident detector flux increases, the output detector voltage increases at a lesser rate. To attain the calibration requirements for these instruments, a correction technique for the detector nonlinearity was implemented. The technique is based on algorithms that were previously developed for AERI instruments and therefore represents a general approach that works for multiple instruments. (The detector nonlinearities for AERI detectors are an order of magnitude smaller than those for the NAST-I and S-HIS.)

Using the predicted behavior of HgCdTe detectors, and following the approaches of Revercomb *et al.* (1994) and Abrams *et al.* (1994), the out-of-band

signal is used to determine the qualitative nature of the nonlinearity. Both detectors on both the NAST-I and S-HIS exhibit a response that is largely quadratic. Therefore, the measured interferogram signal, I_m , is related to the true, corrected linear signal, I_c , by

$$I_c = I_m + a_2(I_m)^2 \quad (1)$$

Separating the measured interferograms into AC $[f(x)]$ and DC (V) components gives

$$I_c = (f+V) + a_2(F+V)^2 \quad (2)$$

For each scene view (raw interferogram), the DC level is modeled as a sum of contributions of incident radiation on the detector from the scene, the unmodulated background, and the instrument emission from both interferometer ports,

$$V = \frac{f_s(0)}{e} + \frac{f_a(0)}{e} \frac{k + 2r_{dw}}{[B(T_a)/B(T_i)](1 - r_{fw}) + r_{fw} - r_{dw}} \quad (3)$$

where $f_s(0)$ and $f_a(0)$ are the interferogram signals at zero path difference of the scene and ambient blackbody views, e is the modulation efficiency, k is the fraction of the detector field-of-view that is modulated, and r_{dw} and r_{fw} are the reflectances of the dewar and front windows. The detector nonlinearity is then characterized by determining the coefficient, a_2 , which represents the quadratic response of the detector.

3.1 NAST-I Detector Nonlinearity

For NAST-I, a_2 has been determined using different approaches: 1) by comparing ground-based, uplooking clear-sky spectra with coincident AERI spectra, 2) by comparing in-flight, downlooking clear-sky spectra with coincident spectra taken with the HIS aboard the ER-2, and 3) by viewing reference blackbodies in the laboratory at 77 K, 0 K, 295 K, 313 K, and 333 K. All three approaches, and the out-of-band response signal, give values of a_2 which agree to within the measurement and comparison uncertainties. The uncertainty in the final value of a_2 is 10 percent or less. Figure 1 presents an overview of the out-of-band response of NAST-I, and highlights the linear behavior of the shortwave InSb detector versus the quadratic behavior of the HgCdTe bands. Figure 2 presents the comparison to the coincident up-looking spectra with AERI, with the uncorrected NAST-I data ($a_2 = 0$) and the corrected data using the value of $a_2 = 1.46$ determined from the comparison.

3.2 S-HIS Detector Nonlinearity

The nonlinearities of the S-HIS detectors are being characterized in a similar manner. To date, a_2 has been determined by comparing with uplooking clear-sky spectra with coincident AERI spectra. Figure 3 shows the comparison results with uncorrected S-HIS data ($a_2 = 0$) and corrected data using the value of $a_2 = 0.51$.

Figure 4 shows a preliminary comparison using data from CAMEX-3 on 13 September 1998 between the S-HIS and the Line-By-Line Radiative Transfer Model (LBLRTM) (Clough *et al.*, 1992). This flight was designated for clear-sky calibration and validation over Andros Island in the Bahamas. The input to LBLRTM was from a dropsonde launched from NASA's DC-8 aircraft. The S-HIS data was a 5-minute average of nadir spectra bracketing the time of the dropsonde launch. The comparison shown in Figure 4 is for the longwave band and shows excellent agreement between the S-HIS measurements and the LBLRTM calculation, especially in the blowup plot of the CO₂ lines between 730 and 740 cm⁻¹.

4. Conclusions

Brief descriptions of two new aircraft-based instruments are presented. A general technique for correcting for detector nonlinearities is given. This technique has proved successful for various instruments, NAST-I, S-HIS, and AERI. Preliminary data from the S-HIS are presented from the Convection and Moisture Experiment III (CAMEX III), where the S-HIS flew aboard a NASA DC-8 research aircraft. These data include results from a clear-sky calibration and validation flight over Andros Island in the Bahamas. Measurements from the S-HIS are compared with line-by-line radiative transfer

calculations using dropsonde data from the DC-8 as input.

5. References

- Abrams, M.C., Toon, G.C., and Schindler, R.A., Practical Example of the Correction of Fourier Transform Spectra for Detector Nonlinearity, *Appl. Opt.*, **33** 6307-6314, 1994.
- Clough, S.A., M.J. Iacono, and J.L. Moncet: Line-by-line calculations of atmospheric fluxes and cooling rates: Application to water vapor. *J. Geophys. Res.*, **97**, 15761-15785, 1992.
- Cousins, D., and Smith, W.L.: National Polar-Orbiting Operational Environmental Satellite System (NPOESS) Airborne Sounder Testbed-Interferometer (NAST-I), 1999, in preparation.
- Revercomb, H.E., H. Buijs, H.B. Howell, D.D. LaPorte, W.L. Smith, and L.A. Sromovsky: Radiometric calibration of IR Fourier transform spectrometers: solution to a problem with the High-Resolution Interferometer Sounder. *Appl. Opt.*, **27**, 3210-3218, 1988.
- Revercomb, H.E., Techniques for Avoiding Phase and Non-linearity Errors in Radiometric Calibration: A Review of Experience with the Airborne HIS and Ground-based AERI}, paper presented at the 5th International Workshop of Atmospheric Science from Space using Fourier Transform Spectroscopy, Tokyo, Japan, 30 November - 2 December, 1994. (available upon request from Revercomb)

Table 1. S-HIS Instrument Specifications.

Interferometer:		
Type:	Voice Coil Dynamically Aligned Plane mirror (Custom Bomem DA-5)	
Beam Diameter	4.5 cm	
Fringe Counting	¼ wave quadrature, continuous	
Optical path drive	Flex Pivot Porch Swing	±1.037 cm; 4 cm/s
OPD sampling reference	HeNe laser w/ white light at startup	
Angular FOV	40 mrad (full)	
Scan Time	0.5 s (2 spectra per spot)	
Spectral Coverage:		
Four Band Option (3-25 µm):	<u>Coverage</u>	<u>Material</u>
Extra Longwave	19-25 µm, 400-525 cm ⁻¹	HgCdTe
Longwave	10-19 µm, 525-1000 cm ⁻¹	HgCdTe
Midwave	5.5-10 µm, 1000-1800 cm ⁻¹	HgCdTe
Shortwave	3-5.5 µm, 1800-3000 cm ⁻¹	InSb
Three Band Option (3-16 µm)		
Longwave	9-16 µm, 620-1100 cm ⁻¹	HgCdTe
Midwave	5.5-9.9 µm, 1100-1800 cm ⁻¹	HgCdTe
Shortwave	3-5.5 µm, 1800-3000 cm ⁻¹	InSb
Spectral Resolution:	0.5 cm ⁻¹	
Spatial Field-of-view:		
Instrument Field-of-view	100 mrad (nadir: 2 km from 20 km altitude)	
Cross Track Scan Step	0.15 rad	programmable
Number of IFOV per scan	11 earth views + 2 calibration views	Programmable
Dwell time per spot	1 s	Programmable
Total scan time	15 s	Programmable
Cooler/Temperature:	0.6 W Stirling Cooler (Litton), 68 K	
Mass/Size:	70 kg; 0.05 m ³	
Power:	225 W	
Onboard processing:	DSP numerical filters	
RMS noise (per spot):	<0.25K at 260 K; except ELW	
Radiometric Calibration:	<0.1K at 260 K; absolute <0.2K at 260 K; reproducibility	

Table 2. NAST-I Instrument Specifications

Interferometer Characteristics:		
Longwave	15.5-7.7 µm, 645-1300 cm ⁻¹	HgCdTe
Midwave	7.7-5.0 µm, 1290-2000 cm ⁻¹	HgCdTe
Shortwave	5.0-3.7 µm, 1980-2700 cm ⁻¹	InSb
Beamsplitter/Compensator	KBr, 1.9 inch clear aperture	
Alignment	Dynamic based on axial HeNe laser	
Optical Path Difference (OPD)	±2 cm or ±0.8 cm, selectable	
OPD velocity	< 11 cm/s in 8 selectable modes	
Input optics field-of-view	7.5 degree circular	
Input optics magnification	For a 2.6 km nadir ground footprint	
Input aperture	6.9 0.8 cm	
Spatial characteristics:		
Instrument field-of-view	7.5 degrees	
	<u>Low resolution mode</u>	<u>High resolution mode †</u>
Scan time:	12.32 s	12.32 s
Field of Regard:	±48.2 deg	±48.2 deg
Step/scan:	15	15
Step Time:	0.821 s	0.821 s
OPD velocity:	5.19 cm/s	2.08 cm/s
Sample rate/band	82.0 Ksam/s	32.9 Ksam/s
Mass:	280 lb	
Power:	970 W	

(†: refers to abutted field-of-view; see Cousins and Smith, 1999)

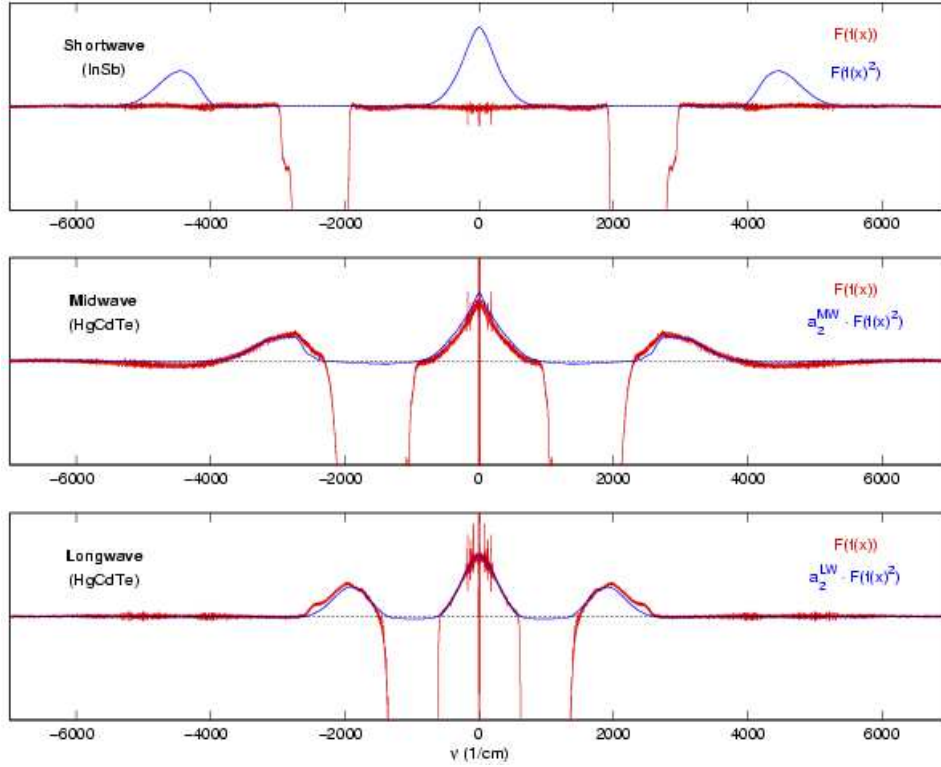


Figure 1. NAST-I interfergrams plotted with the square of the interferograms, illustrating the out-of-band detector response for the shortwave, midwave, and longwave detectors.

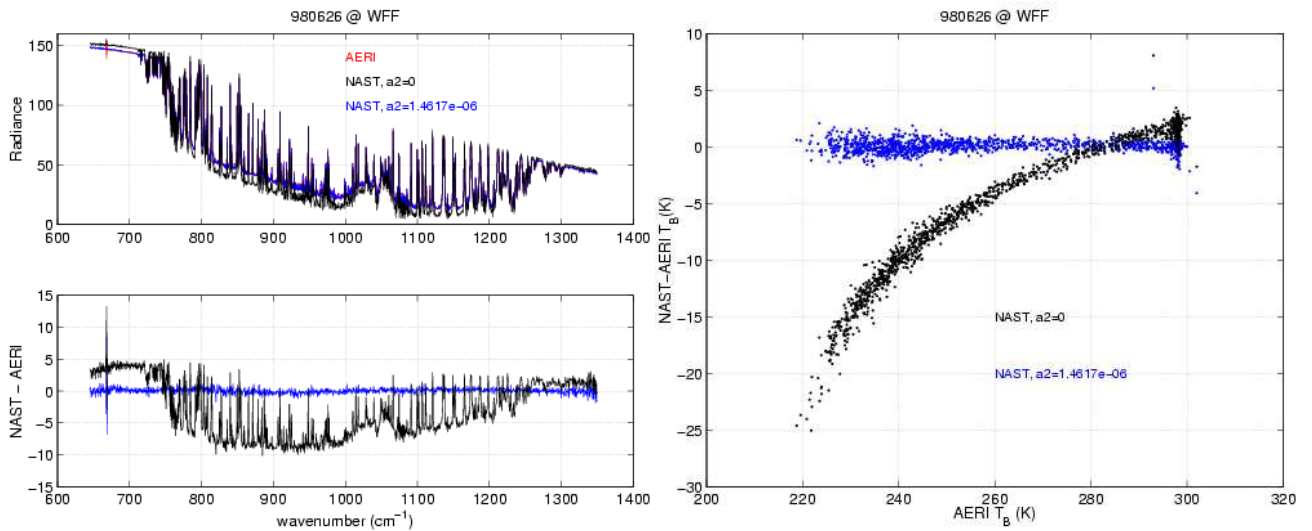


Figure 2. NAST-I nonlinearity correction derived from comparison with a reference AERI instrument. Data were taken at Wallops Flight Facility on 26 June 1998.

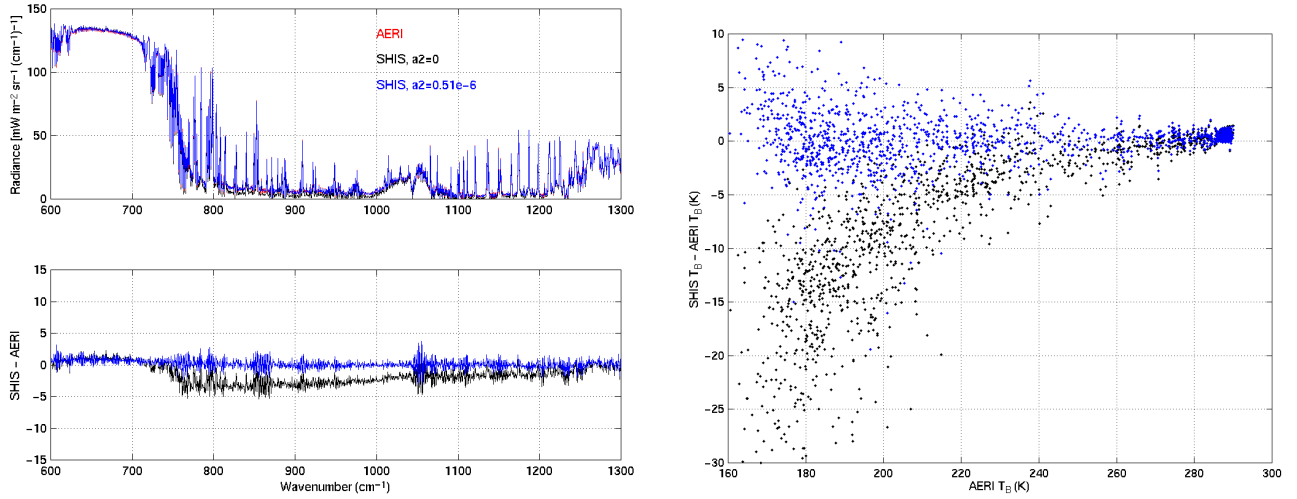


Figure 3. S-HIS nonlinearity correction derived from comparison with a reference AERI instrument. Data were taken in Madison, Wisconsin on 28 October 1998. The spread of brightness temperatures is larger for the S-HIS compared to the NAST-I in Figure 2 because of the lower window radiances experienced on this day compared to 26 June 1998 at Wallops.

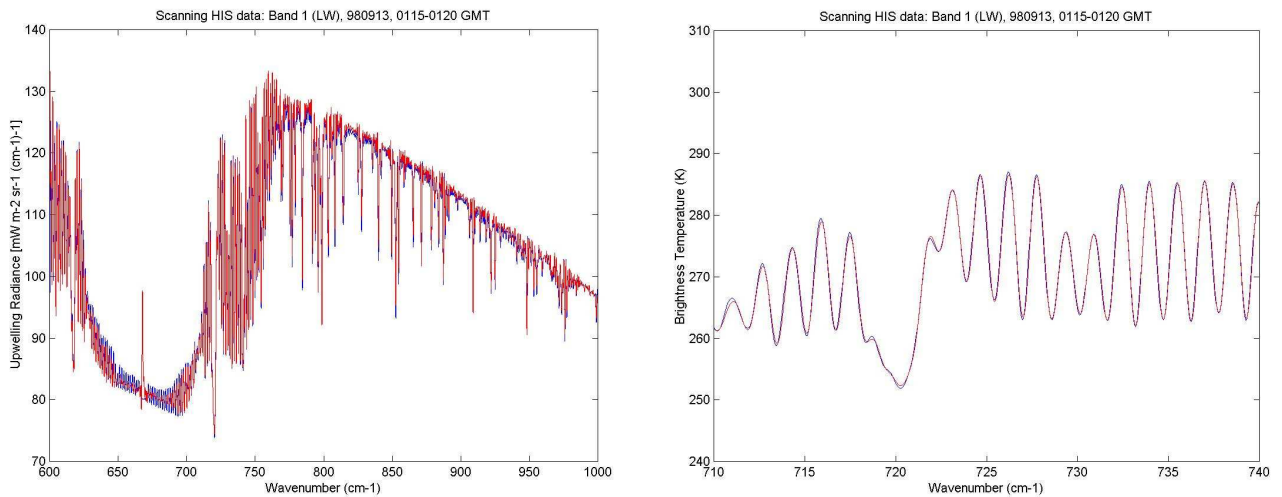


Figure 4. Preliminary comparison of S-HIS data (red) and an LBLRTM calculation (blue). Data were taken near Andros Island in the Bahamas during the CAMEX-3 field experiment.